PRAMANA
— journal of
physics

Vol. 56, No. 1
January 2001
pp. 57–76

Study of $\Lambda\Lambda$ dynamics and ground state structure of low and medium mass double Λ hypernuclei

MD ABDUL KHAN and TAPAN KUMAR DAS
Department of Physics, University of Calcutta, 92, Acharya Prafulla Chandra Road,
Calcutta 700 009, India
Email: tkdas@cucc.ernet.in

MS received 6 April 2000; revised 13 September 2000

Abstract. We critically review the $\Lambda\Lambda$ dynamics by examining $\Lambda-\Lambda$ and Λ-nucleon phenomenological potentials in the study of the bound state properties of double-Λ hypernuclei ${}^{6}_{\Lambda\Lambda}$He, ${}^{10}_{\Lambda\Lambda}$Be, ${}^{14}_{\Lambda\Lambda}$C, ${}^{18}_{\Lambda\Lambda}$O, ${}^{22}_{\Lambda\Lambda}$Ne, ${}^{26}_{\Lambda\Lambda}$Mg, ${}^{30}_{\Lambda\Lambda}$Si, ${}^{34}_{\Lambda\Lambda}$S, ${}^{38}_{\Lambda\Lambda}$Ar, ${}^{42}_{\Lambda\Lambda}$Ca, ${}^{46}_{\Lambda\Lambda}$Ti, ${}^{50}_{\Lambda\Lambda}$Cr, ${}^{54}_{\Lambda\Lambda}$Fe, ${}^{58}_{\Lambda\Lambda}$Ni, ${}^{62}_{\Lambda\Lambda}$Zn, ${}^{66}_{\Lambda\Lambda}$Ge, ${}^{70}_{\Lambda\Lambda}$Se, ${}^{74}_{\Lambda\Lambda}$Kr, ${}^{78}_{\Lambda\Lambda}$Sr, ${}^{82}_{\Lambda\Lambda}$Zr, ${}^{86}_{\Lambda\Lambda}$Mo, ${}^{90}_{\Lambda\Lambda}$Ru, ${}^{94}_{\Lambda\Lambda}$Pd, ${}^{98}_{\Lambda\Lambda}$Cd, ${}^{102}_{\Lambda\Lambda}$Sn in the frame work of (core+Λ+Λ) three body model. An effective ΛN potential is obtained by folding the phenomenological ΛN potential into the density distribution of the core nuclei. The former two cases (i.e. ${}^{6}_{\Lambda\Lambda}$He and ${}^{10}_{\Lambda\Lambda}$Be) are revisited to justify the correctness of the present potential model. Assuming the same potential model we predicted some of the structural properties of heavier doubly Λ-hypernuclei. The hyperspherical harmonics expansion method, which is an essentially exact method has been employed for the three body system. A convergence in binding energy up to 0.15% for $K_{\max} = 20$ has been achieved. In our calculation we have made no approximation in restricting the allowed l-values of the interacting pairs.

Keywords. Hypernuclei; Raynal Revai coefficient; hyperspherical harmonics expansion; hyperspherical harmonics.

PACS Nos 21.80.+a; 21.60.Jz; 21.30.Fe

1. Introduction

The study of the structure of light exotic hypernuclei have become an area of particular interest since the discovery of this species in the early sixties [1–3]. Important members of this new species are the nuclei ${}^{6}_{\Lambda\Lambda}$He, ${}^{10}_{\Lambda\Lambda}$Be and ${}^{13}_{\Lambda\Lambda}$B [1–4]. Discovery of these doubly Λ-hypernuclei opened a new avenue to extract important informations about the $\Lambda-\Lambda$ interaction. Again since hyperons as well as nucleons both have qqq structure (eg. $p \to uud, n \to udd, \Lambda^0 \to uds$ etc., where u, d, s are up, down and strange quark respectively), their interaction among themselves as well as with nucleons should give important inputs in the knowledge of strong interactions (qq interactions). This in turn enhances the range of one's imagination on the possible existence of multistrange hypernuclei and derivation of true hyperon–hyperon and hyperon–nucleon interactions. In the early stages,

the emulsion experiments provided a source of information on hypernuclei, which was limited to binding energies of Λ-particle in the light hypernuclei and the decay rates (lifetimes) [2]. The binding energy data provided physicists some qualitative informations about the Λ-nucleon ($\Lambda-N$) interaction and single particle potential strength for Λ-particle in hypernuclei [5]. The hyperon nucleon scattering experiments have also been performed but these are still in the primary stages and do not provide detailed phase shifts to construct the potential reliably. Some $\Lambda-N$ and $\Sigma-N$ total cross-sections and very few angular distribution at low energies have been measured [6–11], but are not sufficient to allow the phase shift analysis. Nevertheless, the bound state properties of single and double Λ hypernuclei can give valuable indirect information about $\Lambda-N$ and $\Lambda-\Lambda$ interactions. One can, for example, take phenomenological forms of ΛN and $\Lambda\Lambda$ interactions and see if they reproduce the observables of the hypernuclei. Alternatively one can adjust the parameters of the empirical potential to reproduce the bound state properties and thus predict the effective ΛN and $\Lambda\Lambda$ interactions. Earlier attempts in this direction [12–16] used variational and approximate few body calculations for the hypernucleus treated as a few body system. In the present work, we test our potential model (ie, the $\Lambda\Lambda$ and the effective ΛN potential which we obtained by folding the phenomenological ΛN potential into the density distribution of the core nuclei) by studying the general state properties of double Λ-hypernuclei ${}^{6}_{\Lambda\Lambda}$He and ${}^{10}_{\Lambda\Lambda}$Be for which the ground state binding energy is known experimentally. We then apply our potential model to investigate the ground state structural properties of doubly Λ-hypernuclei ${}^{14}_{\Lambda\Lambda}$C, ${}^{18}_{\Lambda\Lambda}$O, ${}^{22}_{\Lambda\Lambda}$Ne, ${}^{26}_{\Lambda\Lambda}$Mg, ${}^{30}_{\Lambda\Lambda}$Si, ${}^{34}_{\Lambda\Lambda}$S, ${}^{38}_{\Lambda\Lambda}$Ar, ${}^{42}_{\Lambda\Lambda}$Ca, ${}^{46}_{\Lambda\Lambda}$Ti, ${}^{50}_{\Lambda\Lambda}$Cr, ${}^{54}_{\Lambda\Lambda}$Fe, ${}^{58}_{\Lambda\Lambda}$Ni, ${}^{62}_{\Lambda\Lambda}$Zn, ${}^{66}_{\Lambda\Lambda}$Ge, ${}^{70}_{\Lambda\Lambda}$Se, ${}^{74}_{\Lambda\Lambda}$Kr, ${}^{78}_{\Lambda\Lambda}$Sr, ${}^{82}_{\Lambda\Lambda}$Zr, ${}^{86}_{\Lambda\Lambda}$Mo, ${}^{90}_{\Lambda\Lambda}$Ru, ${}^{94}_{\Lambda\Lambda}$Pd, ${}^{98}_{\Lambda\Lambda}$Cd, ${}^{102}_{\Lambda\Lambda}$Sn (for which the experimental data is not available treating them each as core+$\Lambda+\Lambda$ three body system. The binary core-Λ subsystem possesses the bound state while no $\Lambda\Lambda$-bound state has been reported). We employ hyperspherical harmonics expansion (HHE) method to solve such a three body system. This method is a powerful tool for the $ab\ initio$ solution of the few body Schrödinger equation for a given set of interaction potentials among the constituent particles. This method has been used for bound states in atomic [17–34], nuclear [35–46] and particle physics [47–49]. Attempts have been made to use it in scattering problems as well [50]. In this method, the wave function is expanded in a complete set of hyperspherical harmonics (HH), which are, for a three body system, the six-dimensional analogue of ordinary spherical harmonics, which are the angular part of eigenfunctions of 3-dimensional Laplacian operator. The resulting Schrödinger equation is a set of coupled differential equations which are solved numerically by the renormalized Numerov method (RNM) [51,52]. The HHE method is essentially an exact one and more reliable than others. It involves no approximation other than an eventual truncation of the expansion basis. By gradually expanding the expansion basis and checking the rate of convergence any desired precision in the binding energy can, in principle, be achieved. However the number of coupled differential equations and therefore the complexity in the numerical solution increases rapidly as the expansion basis is increased by including larger hyper angular momentum quantum numbers. Computer limitations set an ultimate limit to the precision attainable. Thus in this approach the attainment of desired convergence in physical observables are of great importance.

In the present calculation we achieved a convergence in the binding energy to within 0.25%. In addition to the two-Λ separation energy ($B_{\Lambda\Lambda}$) and $\Lambda\Lambda$ bond energy ($\Delta B_{\Lambda\Lambda}$) which are defined as

$$B_{\Lambda\Lambda}({}^{A}_{\Lambda\Lambda}Z) = [M({}^{A-2}Z) + 2M_{\Lambda} - M({}^{A}_{\Lambda\Lambda}Z)]c^2 \tag{1}$$

and

$$\Delta B_{\Lambda\Lambda} = B_{\Lambda\Lambda}({}^{A}_{\Lambda\Lambda}Z) - 2B_{\Lambda}({}^{A-1}_{\Lambda}Z), \tag{2}$$

we have also studied the size, density distribution and correlation among the core and the valence Λ-hyperons.

This paper is organized as follows: In §2, we review the HHE method for a three body system consisting of non identical particles. Results of calculation and discussion are presented in §3. Finally in §4 we draw our conclusions.

2. HHE method

We label the core as particle no '1' and the two valence Λ particles as particles '2' and '3' respectively (see figure 1). For pairwise interactions, we can treat any one of the three particles as the spectator, remaining two being the interacting pair. Thus there are three possible partitions labelled i $(i = 1, 2, 3)$. In the partition i, particle numbered i is the spectator and particles numbered j and k form the interacting pair $(i, j, k = 1, 2, 3,$ cyclic$)$. Now for a given partition i, the Jacobi co-ordinates (which are proportional to the relative separation between the interacting pair and the relative separation between the spectator and the centre of mass of the interacting pair respectively) are defined as:

$$\left.\begin{array}{rcl} \vec{x_i} & = & a_{jk}\,(\vec{r_j} - \vec{r_k}) \\ \vec{y_i} & = & a_{(jk)i}\left(\vec{r_i} - \frac{m_j\vec{r_j} + m_k\vec{r_k}}{m_j + m_k}\right) \\ \vec{R} & = & \frac{1}{M}\,(m_i\vec{r_i} + m_j\vec{r_j} + m_k\vec{r_k}) \end{array}\right\}. \tag{3}$$

The co-efficients a_{jk} and $a_{(jk)i}$ are defined as $a_{jk} = \left[\frac{m_j m_k M}{m_i(m_j+m_k)^2}\right]^{\frac{1}{4}}$ and $a_{(jk)i} = \left[\frac{m_i(m_j+m_k)^2}{m_j m_k M}\right]^{\frac{1}{4}}$ $(i, j, k = 1, 2, 3$ cyclic$)$ where m_i, $\vec{r_i}$ are the mass and position of the ith particle, $M = m_i + m_j + m_k$ is the total mass and $\vec{R}$ is the centre of mass of the system. The sign of $\vec{x_i}$ is fixed by the condition that i, j, k form a cyclic permutation of $(1, 2, 3)$. In the transformation (3) the six dimensional volume element is conserved

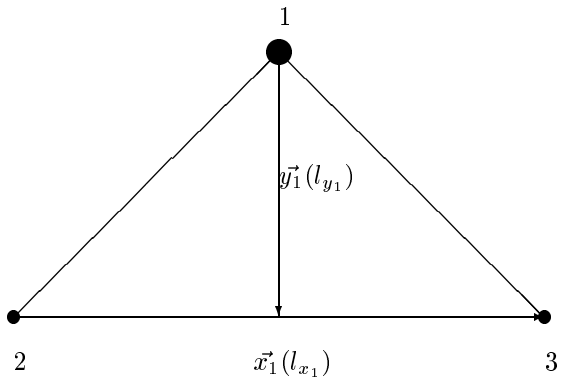

Figure 1. Choice of Jacobi coordinates for the partition 1.

(i.e. the Jacobian is unity) and the centre of mass motion is automatically separated. The relative motion of the three body system is described by the Schrödinger equation

$$\left[-\frac{\hbar^2}{2\mu}(\nabla^2_{x_i}+\nabla^2_{y_i})+V_{jk}(\vec{x_i})+V_{ki}(\vec{x_i},\vec{y_i})+V_{ij}(\vec{x_i},\vec{y_i})-E\right]\Psi(\vec{x_i},\vec{y_i})=0, \quad (4)$$

where $\mu = \left[\frac{m_i m_j m_k}{M}\right]^{\frac{1}{2}}$ is an effective mass parameter and V_{ij} is the interaction potential between ith and jth particles. We next introduce the hyperspherical variables defined by [46]

$$\left.\begin{array}{rcl} x_i &=& \rho\cos\phi_i \\ y_i &=& \rho\sin\phi_i \end{array}\right\}, \quad (5)$$

where $\rho = \sqrt{x_i^2+y_i^2}$ is the global length (also called the hyper radius), which is invariant under three dimensional rotations and permutations of the particle indices. Thus ρ is the same for all three partitions. The five other hyperspherical variables include the hyperspherical angle $\phi_i = \tan^{-1}(y_i/x_i)$ and the polar angles (θ_{x_i}, ϕ_{x_i}) and (θ_{y_i}, ϕ_{y_i}) giving orientations of $\vec{x_i}$ and $\vec{y_i}$ respectively. These are collectively denoted by

$$\Omega_i \equiv \{\phi_i, \theta_{x_i}, \phi_{x_i}, \theta_{y_i}, \phi_{y_i}\} \quad (6)$$

and are called the 'hyperangles'. The six dimensional volume element is given by

$$\mathrm{d}V_6 = \rho^5\,\mathrm{d}\rho\,\cos^2\phi_i\,\sin^2\phi_i\,\mathrm{d}\phi_i\mathrm{d}\Omega_{x_i}\mathrm{d}\Omega_{y_i}, \quad (7)$$

where

$$\left.\begin{array}{rcl} \mathrm{d}\Omega_{x_i} &=& \sin\theta_{x_i}\,\mathrm{d}\theta_{x_i}\,\mathrm{d}\phi_{x_i} \\ \mathrm{d}\Omega_{y_i} &=& \sin\theta_{y_i}\,\mathrm{d}\theta_{y_i}\,\mathrm{d}\phi_{y_i} \end{array}\right\}. \quad (8)$$

In terms of the hyperspherical variables the Schrödinger equation becomes

$$\left[-\frac{\hbar^2}{2\mu}\left\{\frac{1}{\rho^5}\frac{\partial}{\partial\rho}\left(\rho^5\frac{\partial}{\partial\rho}\right)-\frac{\hat{\mathcal{K}}^2(\Omega_i)}{\rho^2}\right\}+V(\rho,\Omega_i)-E\right]\Psi(\rho,\Omega_i) = 0, \quad (9)$$

where $V(\rho,\Omega_i)$ = $V_{jk}(\vec{x_i})+V_{ki}(\vec{x_i},\vec{y_i})+V_{ij}(\vec{x_i},\vec{y_i})$ is the total interaction potential expressed in terms of the hyperspherical variables and $\hat{\mathcal{K}}^2(\Omega_i)$ is the square of hyper angular momentum operator given by [46]

$$\hat{\mathcal{K}}^2(\Omega_i) = -\frac{\partial^2}{\partial{\phi_i}^2}-4\cot 2\phi_i\,\frac{\partial}{\partial\phi_i}+\frac{1}{\cos^2\phi_i}\hat{l}^2(\hat{x_i})+\frac{1}{\sin^2\phi_i}\hat{l}^2(\hat{y_i}), \quad (10)$$

where $\hat{l}^2(\hat{x_i})$ and $\hat{l}^2(\hat{y_i})$ are the squares of ordinary orbital angular momentum operators associated with $\vec{x_i}$ and $\vec{y_i}$ motions. The operator $\hat{\mathcal{K}}^2$ satisfies an eigenvalue equation [46]

$$\hat{\mathcal{K}}^2(\Omega_i)\mathcal{Y}_{K\alpha_i}(\Omega_i) = K(K+4)\mathcal{Y}_{K\alpha_i}(\Omega_i), \quad (11)$$

where α_i is an abbreviation for the set of four quantum numbers $\{l_{x_i}, l_{y_i}, L, M\}$ and K, the hyper angular momentum quantum number (which is not a conserved quantity for the

3-body system) is given by $K = 2n_i + l_{x_i} + l_{y_i}$ (n_i being a non negative integer). The quantity K is the degree of the homogeneous harmonic polynomials $\rho^K \mathcal{Y}_{K\alpha_i}(\Omega_i)$ in the cartesian components of $\vec{x_i}$ and $\vec{y_i}$. Note that the quantum number K is invariant under the change of partition and hence does not involve the partition label. The eigen function of $\hat{\mathcal{K}}^2$ are called hyperspherical harmonics (HH) and are given by

$$\mathcal{Y}_{K\alpha_i}(\Omega_i) = {}^{(2)}P_K{}^{l_{y_i}\ l_{x_i}}(\phi_i)\left[Y_{l_{x_i}}(\hat{x_i})\ Y_{l_{y_i}}(\hat{y_i})\right]_{LM}, \tag{12}$$

where

$$\begin{aligned} {}^{(2)}P_K{}^{l_{y_i}\ l_{x_i}}(\phi_i) &= N_K{}^{l_{x_i},\ l_{y_i}}\ (\cos\ \phi_i)^{l_{x_i}} \\ &\quad \times (\sin\ \phi_i)^{l_{y_i}}\ P_{n_i}{}^{l_{y_i}+1/2,\ l_{x_i}+1/2}\ (\cos\ 2\phi_i). \end{aligned} \tag{13}$$

The normalization constant $N_K^{l_{x_i},l_{y_i}}$ is given by

$$N_K^{l_{x_i},L_{y_i}} \ = \ \left[\frac{2\ n_i!(K+2)(n_i\ +\ l_{x_i}\ +\ l_{y_i}\ +\ 1)!}{\Gamma(n_i\ +\ l_{x_i}\ +\ 3/2)\ \Gamma(n_i\ +\ l_{y_i}+3/2)}\right]^{\frac{1}{2}} \tag{14}$$

and $P_n^{\alpha,\beta}(x)$ is the Jacobi polynomial [53]. The HH's $\{\mathcal{Y}_{K\alpha_i}(\Omega_i)\}$ form a complete orthonormal set in the angular hyperspace (Ω_i).

In the present method the wave function $\Psi(\rho, \Omega_i)$ is expanded in the complete set of HH corresponding to a given partition (say partition i):

$$\Psi(\rho, \Omega_i) = \sum_{K\alpha_i} \frac{U_{K\alpha_i}(\rho)}{\rho^{5/2}} \mathcal{Y}_{K\alpha_i}(\Omega_i). \tag{15}$$

The hyper radial phase factor $\rho^{-5/2}$ is included in order to remove the first order derivative with respect to ρ in eq. (9). Substitution of eq. (15) in eq. (9) and the use of orthonormality of HH leads to a set of coupled differential equations (CDE) in ρ

$$\begin{aligned} &\left[-\tfrac{\hbar^2}{2\mu}\left(\tfrac{\mathrm{d}^2}{\mathrm{d}\rho^2} - \tfrac{\mathcal{L}_K(\mathcal{L}_K+1)}{\rho^2}\right) - E\right] U_{K\alpha_i}(\rho) \\ &+\ \textstyle\sum_{K'\alpha_i'} \langle K\alpha_i \mid V(\rho,\Omega_i) \mid K'\alpha_i'\rangle U_{K'\alpha_i'}(\rho)\ =\ 0, \end{aligned} \tag{16}$$

where $\mathcal{L}_K = K + 3/2$ and

$$\langle K\alpha_i | V(\rho,\Omega_i) | K'\alpha_i'\rangle = \int_{\Omega_i} \mathcal{Y}^*_{K\alpha_i}(\Omega_i) V(\rho,\Omega_i) \mathcal{Y}_{K'\alpha_i'}(\Omega_i) \mathrm{d}\Omega_i. \tag{17}$$

Since the expansion (15) is, in principle, an infinite one, the CDE, eq. (16) is also an infinite set. For practical purposes, the expansion (15) has to be truncated to a finite set, leading to a finite set of CDE. Restrictions arising out of symmetry requirement and imposition of conserved quantum numbers (e.g., total angular momentum, parity etc.) can reduce the expansion basis further and consequently a smaller set of CDE is to be solved.

Evaluation of the matrix elements of the type $\langle \mathcal{Y}_{K\alpha_i}(\Omega_i) | V_{jk}(x_i) | \mathcal{Y}_{K'\alpha_i'}(\Omega_i)\rangle$ (for central interactions) are straight forward, while those for the matrix elements of the type $\langle \mathcal{Y}_{K\alpha_i}(\Omega_i) | V_{ki}(x_j) | \mathcal{Y}_{K'\alpha_i'}(\Omega_i)\rangle$ and $\langle \mathcal{Y}_{K\alpha_i}(\Omega_i) | V_{ij}(x_k) | \mathcal{Y}_{K'\alpha_i'}(\Omega_i)\rangle$ become very

complicated even for central interactions, since both $\vec{x_j}$ or $\vec{x_k}$ are expressed as linear combinations of $\vec{x_i}$ and $\vec{y_i}$, hence $\vec{x_j}$ and $\vec{x_k}$ depend on the polar angles of $\vec{x_i}$ and $\vec{y_i}$ (i.e. $\hat{x_i}$, $\hat{y_i}$) (see eq. (3)). But the calculation of these matrix elements will be quite simple in the partitions j or k respectively, since in these partitions $\vec{x_j}$ or $\vec{x_k}$ are independent of $\vec{y_j}$ and $\vec{y_k}$ respectively. Since the choice of a particular partition is arbitrary, the HH basis corresponding to any chosen partition i forms a complete set spanning the same hyper angular space. One can then relate the HH basis for two different partitions i and j through a unitary transformation. Then a particular element, $\mathcal{Y}_{K\alpha_i}(\Omega_i)$ in the partition i can be expanded in the HH basis corresponding to partition j as:

$$\mathcal{Y}_{K\alpha_i}(\Omega_i) \;=\; \sum_{l_{x_j} l_{y_j}} \langle l_{x_i} l_{y_i} \mid l_{x_j} l_{y_j} \rangle_{KL} \mathcal{Y}_{K\alpha_j}(\Omega_j), \tag{18}$$

where the transformation coefficients $\langle l_{x_i} l_{y_i} \mid l_{x_j} l_{y_j} \rangle_{KL}$ are called the Raynal Revai coefficients (RRC) [54]. Since K, L and M are independent of the partition, the sum is over l_{x_j} and l_{y_j} only, subject to the restrictions $\vec{l_{x_i}} + \vec{l_{y_i}} = \vec{L} = \vec{l_{x_j}} + \vec{l_{y_j}}$. These coefficients can be computed easily [34]. Since the RRC's do not involve ρ, these are calculated once only and stored and it reduces the CPU time significantly.

In terms of the RRC's the matrix elements of V_{ki} in the partition i can be written as

$$\begin{aligned}\langle \mathcal{Y}_{K\alpha_i}(\Omega_i) \mid V_{ki}(x_j) \mid \mathcal{Y}_{K'\alpha_i'}(\Omega_i) \rangle = & \sum_{l'_{x_j} l'_{y_j} l_{x_j} l_{y_j}} \langle l_{x_i} l_{y_i} \mid l_{x_j} l_{y_j} \rangle^*_{KL} \\ & \times \langle l'_{x_i} l'_{y_i} \mid l'_{x_j} l'_{y_j} \rangle_{K'L} \\ & \times \langle \mathcal{Y}_{K\alpha_j}(\Omega_j) \mid V_{ki}(x_j) \mid \mathcal{Y}_{K'\alpha_j'}(\Omega_j) \rangle. \end{aligned} \tag{19}$$

The matrix element on the right side of eq. (19) has the same form as the matrix element of V_{jk} in the partition i (preferred partition) and can be evaluated in a simple way. Thus computing the RRC's involved in eq. (19), the matrix element of V_{ki} in the partition i can be evaluated easily. Similar technique can be employed for the calculation of the matrix element of V_{ij}.

Calculation of potential matrix elements in the preferred partition (in which the pair interaction potential is a function only of the corresponding $\vec{x}$ of the partition) can be further simplified by introducing a multipolar expansion [35] of the potential. For a matrix element in the preferred partition, say partition i, the potential $V_{jk}(x_i)$, is expanded in an appropriate subset of corresponding HH,

$$V_{jk}(x_i) = \sum_{K''\alpha_i''} v^{(jk)}_{K''\alpha_i''}(\rho) \mathcal{Y}_{K''\alpha_i''}(\Omega_i), \tag{20}$$

where $v^{(jk)}_{K''\alpha_i''}(\rho)$ is called the potential multipole and can be evaluated by the use of orthonormality of HH:

$$v^{(jk)}_{K''\alpha_i''}(\rho) = \int V_{jk}(x_i) \mathcal{Y}^*_{K''\alpha_i''}(\Omega_i) \mathrm{d}\Omega_i. \tag{21}$$

The matrix element thus becomes

$$\langle \mathcal{Y}_{K\alpha_i}(\Omega_i) \mid V_{jk}(x_i) \mid \mathcal{Y}_{K'\alpha_i'}(\Omega_i) \rangle = \sum_{K''\alpha_i''} v^{(jk)}_{K''\alpha_i''}(\rho) \langle K\alpha_i \mid K''\alpha_i'' \mid K'\alpha_i' \rangle, \tag{22}$$

where

$$\langle K\alpha_i \mid K''\alpha_i'' \mid K'\alpha_i'\rangle = \int \mathcal{Y}^*_{K\alpha_i}(\Omega_i)\mathcal{Y}_{K''\alpha_i''}(\Omega_i)\mathcal{Y}_{K'\alpha_i'}(\Omega_i)\mathrm{d}\Omega_i \tag{23}$$

is called the geometrical structure coefficients (GSC). These are independent of ρ and the interaction. Hence these coefficients need to be calculated once only and stored resulting in a fast and efficient algorithm. The GSC's involved in eq. (22) will be calculated by standard numerical integration. However they can be calculated in a very elegant manner [55] by using the completeness property of the HH basis. Finally the set of CDE's eq. (16) is to be solved numerically subject to appropriate boundary conditions to get the energy E and the partial waves $U_{K\alpha_i}(\rho)$.

3. Results and discussion

In the present calculation we have taken the core to be structureless. Since the core (^{4}He, ^{8}Be, ^{12}C, ^{16}O, ^{20}Ne, ^{24}Mg, ^{28}Si, ^{32}S, ^{36}Ar, ^{40}Ca, ^{44}Ti, ^{48}Cr, ^{52}Fe, ^{56}Ni, ^{60}Zn, ^{64}Ge, ^{68}Se, ^{72}Kr, ^{76}Sr, ^{80}Zr, ^{84}Mo, ^{88}Ru, ^{92}Pd, ^{96}Cd, ^{100}Sn) contains only nucleons and no Λ-particles, there is no symmetry requirements under exchange of the valence Λ particles with the core nucleons. The only symmetry requirements are (i) antisymmetrization of the core wave function under exchange of the nucleons, and (ii) antisymmetrization of the three body wave function under exchange of the two Λ-particles. The former is implicitly taken care of in the choice of the core as a building block. The latter is correctly incorporated by restricting the l_{x_1} values, as discussed in detail in the following. Thus, within the three body model, the symmetry requirements are correctly satisfied without any approximation. The ground state of all experimentally known double-Λ hypernuclei have a total angular momentum $J = 0$ and positive parity. We assume this to be true for all double-Λ hypernuclei with cores having $N = Z =$ even. The possible total spin (S) of the three body system (core $+\Lambda + \Lambda$) can take two values '0' or '1' since the spin of the core in all the above cases has a value 0. Thus the total orbital angular momentum L can be either 0 or 1 corresponding to $S = 0$ or 1 respectively. Hence the ground state of all the above doubly Λ-hypernuclei is an admixture of the states $^1S_0$ and $^3P_0$. Since the core is spinless, the spin singlet state ($S = 0$) corresponds to zero total spin of the valence Λ-particles (i.e. $S_{23} = 0$). Hence the spin part of the wave function is antisymmetric under the exchange of the spins of the two Λ-particles. Thus the spatial part must be symmetric under the exchange of the two Λ-hyperons. The symmetry of the spatial part is determined by the hyper spherical harmonics, since the hyper radius ρ and hence the hyper radial partial waves ($U_{K\alpha}(\rho)$) are invariant under permutation of the particles. Under the pair exchange operator P_{23} which interchanges particles 2 and 3, $\vec{x_1} \to -\vec{x}_1$ and $\vec{y_1}$ remains unchanged (see eq. (3)). Consequently P_{23} acts like the parity operator for (23) pair only. Choosing the two valence Λ-hyperons to be in spin singlet state (spin antisymmetric), the space wave function must be symmetric under P_{23}. This then requires l_{x_1} to be even. For the spin singlet state total orbital angular momentum, $L = 0$, hence we must have $l_{x_1} = l_{y_1}$ = even integer. Since $K = 2n_1 + l_{x_1} + l_{y_1}$, where n_1 is a non-negative integer, K must be even and

$$\left.\begin{array}{rcl} l_{x_1} = l_{y_1} = & 0,2,4,....,K/2 & \text{if } K/2 \text{ is even} \\ & 0,2,4,....,(K/2-1) & \text{if } K/2 \text{ is odd} \end{array}\right\}. \tag{24}$$

Again for the triplet state ($S = 1$), the two valence Λ-hyperons will be in spin triplet state ($S_{23} = 1$, spin symmetric). Hence the space wave function must be antisymmetric under P_{23}. This then requires l_{x_1} to be odd. For the spin triplet state, the total orbital angular momentum, $L = 1$, hence l_{y_1} may take values l_{x_1} and $l_{x_1} \pm 1$ but the parity conservation allows $l_{y_1} = l_{x_1}$ only. Again since $K = 2n_1 + l_{x_1} + l_{y_1}$, where n_1 is a non-negative integer, K must be even and

$$\left.\begin{array}{rcl} l_{x_1} = l_{y_1} = & 1,3,5,....,K/2 & \text{if } K/2 \text{ is odd} \\ & 1,3,5,....,(K/2-1) & \text{if } K/2 \text{ is even} \end{array}\right\}. \tag{25}$$

For a practical calculation, the HH expansion basis (eq. (15)) is truncated to a maximum value ($K_{\max}$) of K. For each allowed $K \leq K_{\max}$ with K = even integers, all allowed values of $l_{x_1} (= 0, 1, 2, 3, 4, \ldots, K/2)$ are included. The even l_{x_1} values correspond to $L = 0$, $S = 0$ and the odd l_{x_1} values correspond to $L = 1$, $S = 1$. This truncates eq. (16) to a set of N coupled differential equations, where

$$\left.\begin{array}{rcl} N = & \left(\dfrac{K_{\max}}{2}+1\right) & \left(\dfrac{K_{\max}}{4}+1\right) \quad \text{if } K_{\max}/2 \text{ is even} \\ & \left(\dfrac{K_{\max}+2}{4}\right) & \left(\dfrac{K_{\max}}{2}+2\right) \quad \text{if } K_{\max}/2 \text{ is odd} \end{array}\right\}. \tag{26}$$

The truncated set of CDE has been solved by the hyperspherical adiabatic approximation (HAA) [56].

Two body potentials

A number of phenomenological as well as meson-exchange motivated forms were used for the $\Lambda\Lambda$ interaction in earlier attempts. Based on the data available some selection was made between Nijmegen potential models [57,58]. Since knowledge of $\Lambda\Lambda$ scattering is still quite inadequate, it is not possible to establish realistic $\Lambda\Lambda$ potentials at this stage. Instead we adopt here a purely phenomenological strategy. We used the three term Gaussian $\Lambda\Lambda$ potential model D proposed by Nijmegen group [59]. They proposed OBE potential models D and F based on the NN, ΛN and ΣN data along with the SU(3) symmetry. The Nijmegen $D\Lambda - \Lambda$ potential is given by

$$V_{\Lambda\Lambda}(r) = \sum_{i=1}^{3} V_i \exp\left(-\frac{r^2}{\beta_i^2}\right) \tag{27}$$

[58] without any restriction over l values. The parameters of the $\Lambda\Lambda$ interaction are listed in table 1. The core-Λ potential is obtained by folding phenomenological Λ-nucleon potential (assumed one term Gaussian) into the nuclear density distribution of the core which is chosen to have an Wood–Saxon shape given by

Table 1. Parameters of $\Lambda\Lambda$ interaction from [57,58].

$i \rightarrow$	1	2	3
β_i (fm)	1.5	0.9	0.5
V_i (ND)	-8.967	-226.800	880.700

Table 2. Parameters of the $\Lambda-N$ potential and corresponding Λ separation energy in different ${}^{A}_{\Lambda}{}^{-1}Z$ (i.e. core-Λ subsystems).

System	$\Lambda-N$ potential parameters		B_Λ (MeV)	
	V_0 (MeV)	χ (fm)	Experimental	Empirical
${}^{5}_{\Lambda}$He	−71.05	1.034	3.12 ± 0.02 [5]	–
${}^{9}_{\Lambda}$Be	−52.04	1.034	6.71 ± 0.04 [5]	–
${}^{13}_{\Lambda}$C	−50.32	1.034	11.22 ± 0.08 [66]	–
${}^{17}_{\Lambda}$O	−48.88	1.034	–	14.61 ± 1.5
${}^{21}_{\Lambda}$Ne	−45.95	1.034	–	16.24 ± 1.5
${}^{25}_{\Lambda}$Mg	−43.67	1.034	–	17.42 ± 1.5
${}^{29}_{\Lambda}$Si	−41.87	1.034	–	18.32 ± 1.5
${}^{33}_{\Lambda}$S	−40.41	1.034	–	19.04 ± 1.5
${}^{37}_{\Lambda}$Ar	−39.21	1.034	–	19.62 ± 1.5
${}^{41}_{\Lambda}$Ca	−38.19	1.034	–	20.11 ± 1.5
${}^{45}_{\Lambda}$Ti	−37.33	1.034	–	20.53 ± 1.5
${}^{49}_{\Lambda}$Cr	−36.60	1.034	–	20.88 ± 1.5
${}^{53}_{\Lambda}$Fe	−35.92	1.034	–	21.20 ± 1.5
${}^{57}_{\Lambda}$Ni	−35.34	1.034	–	21.47 ± 1.5
${}^{61}_{\Lambda}$Zn	−34.84	1.034	–	21.71 ± 1.5
${}^{65}_{\Lambda}$Ge	−34.37	1.034	–	21.93 ± 1.5
${}^{69}_{\Lambda}$Se	−33.96	1.034	–	22.13 ± 1.5
${}^{73}_{\Lambda}$Kr	−33.60	1.034	–	22.31 ± 1.5
${}^{77}_{\Lambda}$Sr	−33.24	1.034	–	22.47 ± 1.5
${}^{81}_{\Lambda}$Zr	−32.93	1.034	–	22.62 ± 1.5
${}^{85}_{\Lambda}$Mo	−32.65	1.034	–	22.76 ± 1.5
${}^{89}_{\Lambda}$Ru	−32.38	1.034	–	22.89 ± 1.5
${}^{93}_{\Lambda}$Pd	−32.15	1.034	–	23.01 ± 1.5
${}^{97}_{\Lambda}$Cd	−31.90	1.034	–	23.12 ± 1.5
${}^{101}_{\Lambda}$Sn	−31.69	1.034	–	23.22 ± 1.5

$$\rho(r) = \frac{\rho_0}{1 + \exp(\frac{r-c}{a})} \tag{28}$$

with $c = r_0 A_c^{1/3}$ fm, $a = 0.60$ fm, $r_0 = 1.1$ fm (where c is termed the half density radius and a, the skin thickness), and the density constant ρ_0 is determined by the condition

$$\int \rho(r) \mathrm{d}^3 r = A_c, \tag{29}$$

where A_c is the mass of the core in units of nucleon mass. The value of a and r_0 are chosen following suggestions in the literatutre. The phenomenological $\Lambda - N$ potential is given by

$$V_{\Lambda N}(r) = V_0 \exp(-r^2/\chi^2) \tag{30}$$

with V_0 adjusted to reproduce the Λ binding energy (B_Λ) (experimental or empirical, see table 2) in the core-Λ subsystem and $\chi = 1.034$ fm (which is equivalent to two pion exchange Yukawa range). Then the core-Λ potential is given by

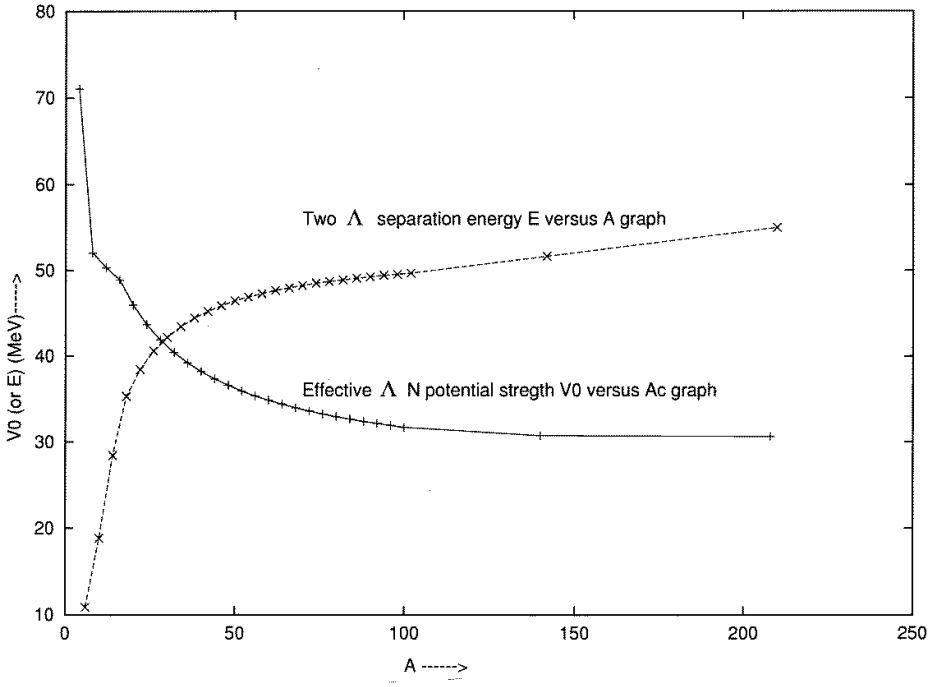

Figure 2. Plot of the strength (V_0) of ΛN effective potential and two-Λ separation energy $B_{\Lambda\Lambda}$ against the mass number A (data taken from tables 2 and 5).

$$V_{c\Lambda}(r) = \int \rho(r_1) V_{\Lambda N}(|\vec{r_1} - \vec{r}|) \mathrm{d}^3 r_1. \tag{31}$$

The strength of ΛN potential is expected to be weakened with the increase in mass of the core due to the screening or shielding effect by neighbouring nucleons within the core when the interacting nucleon is embedded in the core. The π-mesic decay of Λ hyperon ($\Lambda \to N + \pi$) is predominant in the free space but tends to be suppressed in hypernucleus by the Pauli-exclusion principle and instead non-mesic weak process ($\Lambda + N \to N + N$) becomes dominant with increasing mass number [60–65]. Thus we actually get an effective ΛN interaction by the folding process. The parameters of this effective ΛN potential are listed in table 2. A plot of effective ΛN potential strength against mass of the core has been shown in figure 2. As evident from eq. (26) the number of basis states and hence the size of CDE increases rapidly as $K_{\max}$ increases. The truncated set of CDE takes the form

$$\left[-\frac{\hbar^2}{2\mu}\left(\frac{\mathrm{d}^2}{\mathrm{d}\rho^2} - \frac{\mathcal{L}_K(\mathcal{L}_K+1)}{\rho^2}\right) - E\right] U_{K l_{x_1} LS}(\rho)$$
$$+ \sum_{K'=0,2,\ldots}^{K_{\max}} \sum_{l'_{x_1}(\text{allowed})} \sum_{(L'S')=(0,0),(1,1)} \langle K l_{x_1} \mid V(\rho, \Omega_1) \mid K' l'_{x_1} \rangle$$
$$\times\, U_{K' l'_{x_1} L' S'}(\rho) \;=\; 0 \tag{32}$$

(allowed $l'_{x_1} = 0, 2, \ldots$ only for $S = 0$, $L = 0$ otherwise $l'_{x_1} = 1, 3, \ldots$ for $S = 1, L = 1$). Note that the subscripts $l_{y_1} (= l_{x_1})$ or $l'_{y_1} (= l'_{x_1})$ have been suppressed for brevity. The calculated values of binding energy (BE), ΛΛ bond energy ($\Delta B_{\Lambda\Lambda}$) for $K_{\max} = 20$ for the ground state of ${}^{6}_{\Lambda\Lambda}$He, ${}^{10}_{\Lambda\Lambda}$Be, ${}^{14}_{\Lambda\Lambda}$C, ${}^{18}_{\Lambda\Lambda}$O, ${}^{22}_{\Lambda\Lambda}$Ne, ${}^{26}_{\Lambda\Lambda}$Mg, ${}^{30}_{\Lambda\Lambda}$Si, ${}^{34}_{\Lambda\Lambda}$S, ${}^{38}_{\Lambda\Lambda}$Ar, ${}^{42}_{\Lambda\Lambda}$Ca, ${}^{46}_{\Lambda\Lambda}$Ti, ${}^{50}_{\Lambda\Lambda}$Cr, ${}^{54}_{\Lambda\Lambda}$Fe, ${}^{58}_{\Lambda\Lambda}$Ni, ${}^{62}_{\Lambda\Lambda}$Zn, ${}^{66}_{\Lambda\Lambda}$Ge, ${}^{70}_{\Lambda\Lambda}$Se, ${}^{74}_{\Lambda\Lambda}$Kr, ${}^{78}_{\Lambda\Lambda}$Sr, ${}^{82}_{\Lambda\Lambda}$Zr, ${}^{86}_{\Lambda\Lambda}$Mo, ${}^{90}_{\Lambda\Lambda}$Ru, ${}^{94}_{\Lambda\Lambda}$Pd, ${}^{98}_{\Lambda\Lambda}$Cd, ${}^{102}_{\Lambda\Lambda}$Sn are shown in table 5. The empirical Λ-binding energy B_Λ of table 5 has been calculated using the empirical formula

$$B_\Lambda(A) = [(27.0 - 81.9A^{-2/3}) \pm 1.5]\,\mathrm{MeV}, \tag{33}$$

where A is the mass number of the single Λ hypernuclei [5]. The calculated binding energy $B_{\Lambda\Lambda}$ of ${}^{6}_{\Lambda\Lambda}$He agrees fairly well with the experimental value 10.90±0.50 MeV [2] within the experimental error limit. While that for ${}^{10}_{\Lambda\Lambda}$Be is slightly larger than the experimental value 17.7 ± 0.40 MeV [1]. The variation of the calculated two Λ separation energy $B_{\Lambda\Lambda}$ of doubly Λ hypernuclei with mass A has been shown in figure 2. Having obtained the wave function by the HHE approach some of the observables of the three body system have been calculated. These include the root mean square (r.m.s.) radius of the three body system

$$R_A = \left[\frac{A_c R_c^2 + m_\Lambda \langle r_{13}^2 + r_{12}^2\rangle}{A_c + 2m_\Lambda}\right]^{1/2}, \tag{34}$$

where A_c, m_Λ are the masses of the core and the Λ hyperon (in units of nucleon mass) and R_c is the matter radius of the core determined by the relation $R_c = r_0 A_c^{1/3}$ with $r_0 = 1.1$ fm. The r.m.s. core-Λ separation is defined as

$$R_{c\Lambda} = \left[\frac{\langle r_{13}^2 + r_{12}^2\rangle}{2}\right]^{1/2}. \tag{35}$$

The expectation value of the observables $\langle r_{13}^2 + r_{12}^2\rangle$ are obtained by the expression

$$\begin{aligned}\langle r_{13}^2 + r_{12}^2\rangle = & \sum_{KK'l_{x_1}LS} \int_0^\infty \rho^2 \mathrm{d}\rho U_{Kl_{x_1}LS}(\rho) U_{K'l_{x_1}LS}(\rho) \\ & \times \int_0^{\pi/2} {}^{(2)}P_K{}^{l_{x_1},l_{x_1}}(\phi)\, {}^{(2)}P_{K'}{}^{l_{x_1},l_{x_1}}(\phi) \\ & \times \left[\frac{1}{2a_{23}^2}\cos^2\phi + \frac{2}{a_{(23)1}^2}\sin^2\phi\right]\cos^2\phi\sin^2\phi \mathrm{d}\phi. \end{aligned} \tag{36}$$

The r.m.s. separation between the valence Λ-hyperons ($R_{\Lambda\Lambda}$) is given by the expression

$$R_{\Lambda\Lambda} = \left[\langle r_{23}^2\rangle\right]^{1/2}, \tag{37}$$

where

$$\begin{aligned}\langle r_{23}^2\rangle &= \tfrac{1}{a_{23}^2}\textstyle\sum_{KK'l_{x_1}LS} \displaystyle\int_0^\infty \rho^2 \mathrm{d}\rho U_{Kl_{x_1}LS}(\rho) U_{K'l_{x_1}LS}(\rho) \\ &\times \int_0^{\pi/2} {}^{(2)}P_K{}^{l_{x_1},l_{x_1}}(\phi)\ {}^{(2)}P_{K'}{}^{l_{x_1},l_{x_1}}(\phi)\ \cos^4\phi\ \sin^2\phi \mathrm{d}\phi. \end{aligned} \tag{38}$$

The r.m.s. separation between the core (^{4}He, ^{8}Be, ^{12}C etc.) and the C.M. of $\Lambda\Lambda$ pair is given by the expression

$$R_{(\Lambda\Lambda)c} = \left[\langle r^2_{(23)1}\rangle\right]^{1/2}, \tag{39}$$

where

$$\begin{aligned}\langle r^2_{(23)1}\rangle &= \tfrac{1}{a^2_{(23)1}} \textstyle\sum_{KK'l_{x_1}LS} \int_0^\infty \rho^2 \mathrm{d}\rho U_{Kl_{x_1}LS}(\rho) U_{K'l_{x_1}LS}(\rho) \\ &\times \int_0^{\pi/2} {}^{(2)}P_K{}^{l_{x_1},l_{x_1}}(\phi)\ {}^{(2)}P_{K'}{}^{l_{x_1},l_{x_1}}(\phi)\ \cos^2\phi\ \sin^4\phi \mathrm{d}\phi.\end{aligned} \tag{40}$$

The computed value of these r.m.s. radii are listed in tables 3, 4 and 6. In order to study the correlation among the constituent particles (i.e. the core and the valence Λ-hyperons) we computed probability density $P(r_{\Lambda\Lambda}, r_{(\Lambda\Lambda)c})$, where $r_{\Lambda\Lambda} = x_1/a_{23}$ and $r_{(\Lambda\Lambda)c} = y_1/a_{(23)1}$ (see eq. (2)) are respectively the separation between the valence Λ-hyperons and the separation of the core from the centre of mass of the valence Λ-hyperons. The probability density is defined as the probability of finding the three body system having definite separations between the constituent particles. This probability density is given by the expression

$$\begin{aligned}P(r_{\Lambda\Lambda}, r_{(\Lambda\Lambda)c}) = &\sum_{KK'l_{x_1}LS} U_{Kl_{x_1}LS}(\rho) U_{K'l_{x_1}LS}(\rho) {}^{(2)}P_K^{l_{x_1},l_{x_1}}(\phi) \\ &\times {}^{(2)}P_{K'}^{l_{x_1},l_{x_1}}(\phi) \cos^2\phi \sin^2\phi,\end{aligned} \tag{41}$$

with

$$\rho = \left[a^2_{23}\, r^2_{\Lambda\Lambda} + a^2_{(23)1}\, r^2_{(\Lambda\Lambda)c}\right]^{1/2} \tag{42}$$

and

$$\phi = \tan^{-1}\left(\frac{a_{(23)1}}{a_{23}}\,\frac{r_{(\Lambda\Lambda)c}}{r_{\Lambda\Lambda}}\right). \tag{43}$$

A three dimensional plot of $P(r_{\Lambda\Lambda}, r_{(\Lambda\Lambda)c})$ as a function of $r_{\Lambda\Lambda}$ and $r_{(\Lambda\Lambda)c}$ has been shown in figure 3 for $^{10}_{\Lambda\Lambda}$Be hypernuclei as a representative case. The density plot exhibits a cigar-like shape where the valence Λ-hyperons are located on opposite side of the core ($r_{\Lambda\Lambda} > r_{(\Lambda\Lambda)c}$). This can further be confirmed by computing a correlation coefficient defined as

$$\begin{aligned}\eta &= \langle \tfrac{r^2_{(\Lambda\Lambda)c}}{\rho^2}\rangle \\ &= \tfrac{1}{a^2_{(23)1}} \textstyle\sum_{KK'l_{x_1}LS} \int_0^\infty \mathrm{d}\rho U_{Kl_{x_1}LS}(\rho) U_{K'l_{x_1}LS}(\rho) \\ &\times \int_0^{\pi/2} {}^{(2)}P_K{}^{l_{x_1},l_{x_1}}(\phi) {}^{(2)}P_{K'}{}^{l_{x_1},l_{x_1}}(\phi) \\ &\times \cos^2\phi \sin^4\phi \mathrm{d}\phi.\end{aligned} \tag{44}$$

Table 3. Calculated BE $B_{\Lambda\Lambda}$ and r.m.s. radii for different $K_{\max}$ for ${}^{6}_{\Lambda\Lambda}$He hypernucleus.

$K_{\max}$	BE (MeV)	r.m.s. radii (fm)						η
		R_A	$R_{c\Lambda}$	$R_{\Lambda\Lambda}$	$R_{(\Lambda\Lambda)c}$	$R_c^{\rm CM}$	$R_\Lambda^{\rm CM}$	
0	09.09925	2.0747	2.5327	3.1446	1.9856	0.7405	2.0056	0.3157
2	09.41083	2.0535	2.4860	3.1220	1.9348	0.7216	1.9770	0.3158
4	09.85415	2.0507	2.4798	3.0914	1.9391	0.7232	1.9666	0.3187
6	10.16209	2.0360	2.4472	3.0466	1.9153	0.7143	1.9398	0.3209
8	10.41431	2.0262	2.4251	3.0065	1.9030	0.7097	1.9193	0.3237
10	10.59790	2.0208	2.4131	2.9791	1.8985	0.7080	1.9068	0.3263
12	10.72117	2.0187	2.4085	2.9612	1.8996	0.7085	1.9003	0.3285
14	10.79954	2.0185	2.4079	2.9497	1.9034	0.7099	1.8973	0.3302
16	10.85764	2.0191	2.4092	2.9422	1.9079	0.7116	1.8962	0.3315
18	10.87652	2.0199	2.4111	2.9373	1.9122	0.7132	1.8959	0.3323
20	10.89363	2.0207	2.4129	2.9340	1.9158	0.7145	1.8961	0.3329

Table 4. Calculated BE $B_{\Lambda\Lambda}$ and r.m.s. radii for different $K_{\max}$ for ${}^{10}_{\Lambda\Lambda}$Be hypernucleus.

$K_{\max}$	BE (MeV)	r.m.s. radii (fm)						η
		R_A	$R_{c\Lambda}$	$R_{\Lambda\Lambda}$	$R_{(\Lambda\Lambda)c}$	$R_c^{\rm CM}$	$R_\Lambda^{\rm CM}$	
0	16.85281	2.2092	2.2399	2.9556	1.6833	0.3858	1.9665	0.2848
2	17.24068	2.2030	2.2129	2.8655	1.6865	0.3866	1.9345	0.2955
4	17.65940	2.2007	2.2030	2.8394	1.6845	0.3861	1.9239	0.2975
6	18.00125	2.1951	2.1787	2.8016	1.6687	0.3825	1.9017	0.2997
8	18.29194	2.1916	2.1631	2.7698	1.6616	0.3809	1.8863	0.3024
10	18.50776	2.1899	2.1555	2.7468	1.6613	0.3808	1.8777	0.3050
12	18.65403	2.1894	2.1532	2.7308	1.6649	0.3816	1.8738	0.3072
14	18.74717	2.1895	2.1536	2.7198	1.6700	0.3828	1.8725	0.3089
16	18.80392	2.1898	2.1552	2.7124	1.6750	0.3839	1.8724	0.3102
18	18.83741	2.1902	2.1569	2.7073	1.6792	0.3849	1.8729	0.3110
20	18.85670	2.1905	2.1584	2.7039	1.6825	0.3857	1.8734	0.3116

A small value of this coefficient will indicate that the two valence Λ-hyperons are situated on two opposite sides of the core (i.e. a cigar shape when the Λ-hyperons are anti-correlated), while a large value (≤ 1) will indicate the possibility of $\Lambda - \Lambda$ correlation.

The computed values of this coefficient for various three body system is shown in the last column of tables 3, 4 and 6. As the value of η is small ($\sim$0.30), a cigar shape is indicated on the average. Thus, the correlation density plots (figure 3) and the computed value of the correlation coefficient η both indicate that the cigar-like structure are probable. We then computed the partial probability which is the contribution of the orbital angular momenta l_{x_1} to the probability density distribution. This calculation is done at $K_{\max} = 20$ for all the above hypernuclei. The results have been summarized in table 7. Finally we have compared our results with some of the observables calculated by other workers. Yamamoto *et al* [67,68] studied the structure of some light double-Λ hypernuclei in the frame work of core+Λ + Λ three-body model. They used an effective ΛΛ interaction derived from the Nijmegen one boson exchange (OBE) models on the basis of G-matrix calculation and the effective core-Λ interaction used by them was Wood–Saxon one with parameters

Table 5. The calculated Λ binding energy (B_Λ), two Λ separation energy ($B_{\Lambda\Lambda}$) and the $\Lambda\Lambda$ bond energy ($\Delta B_{\Lambda\Lambda}$) for different Λ and double Λ-hypernuclei.

Hypernuclei	B_Λ (MeV)	Hypernuclei	$B_{\Lambda\Lambda}$ (MeV)	$\Delta B_{\Lambda\Lambda}$ (MeV)	$\Delta B_{\Lambda\Lambda}^{\rm Expt.}$ (MeV)
${}^{5}_{\Lambda}$He	3.1214	${}^{6}_{\Lambda\Lambda}$He	10.8936	4.6508	4.7 ± 0.60 [2]
${}^{9}_{\Lambda}$Be	6.7136	${}^{10}_{\Lambda\Lambda}$Be	18.8567	5.4295	4.3 ± 0.40 [1]
${}^{13}_{\Lambda}$C	11.2226	${}^{14}_{\Lambda\Lambda}$C	28.4294	5.9842	–
${}^{17}_{\Lambda}$O	14.6000	${}^{18}_{\Lambda\Lambda}$O	35.3013	6.1013	–
${}^{21}_{\Lambda}$Ne	16.2401	${}^{22}_{\Lambda\Lambda}$Ne	38.4235	5.9433	–
${}^{25}_{\Lambda}$Mg	17.4237	${}^{26}_{\Lambda\Lambda}$Mg	40.5915	5.7441	–
${}^{29}_{\Lambda}$Si	18.3322	${}^{30}_{\Lambda\Lambda}$Si	42.1986	5.5342	–
${}^{33}_{\Lambda}$S	19.0440	${}^{34}_{\Lambda\Lambda}$S	43.4290	5.3410	–
${}^{37}_{\Lambda}$Ar	19.6224	${}^{38}_{\Lambda\Lambda}$Ar	44.4146	5.9547	–
${}^{41}_{\Lambda}$Ca	20.1158	${}^{42}_{\Lambda\Lambda}$Ca	45.1995	4.9679	–
${}^{45}_{\Lambda}$Ti	20.5285	${}^{46}_{\Lambda\Lambda}$Ti	45.8647	4.8077	–
${}^{49}_{\Lambda}$Cr	20.8843	${}^{50}_{\Lambda\Lambda}$Cr	46.4457	4.6771	–
${}^{53}_{\Lambda}$Fe	21.1961	${}^{54}_{\Lambda\Lambda}$Fe	46.8755	4.4833	–
${}^{57}_{\Lambda}$Ni	21.4706	${}^{58}_{\Lambda\Lambda}$Ni	47.2761	4.3349	–
${}^{61}_{\Lambda}$Zn	21.7158	${}^{62}_{\Lambda\Lambda}$Zn	47.6509	4.2193	–
${}^{65}_{\Lambda}$Ge	21.9335	${}^{66}_{\Lambda\Lambda}$Ge	47.9443	4.0773	–
${}^{69}_{\Lambda}$Se	22.1301	${}^{70}_{\Lambda\Lambda}$Se	48.2266	3.9664	–
${}^{73}_{\Lambda}$Kr	22.3090	${}^{74}_{\Lambda\Lambda}$Kr	48.4987	3.8807	–
${}^{77}_{\Lambda}$Sr	22.4731	${}^{78}_{\Lambda\Lambda}$Sr	48.6885	3.7423	–
${}^{81}_{\Lambda}$Zr	22.6240	${}^{82}_{\Lambda\Lambda}$Zr	48.8931	3.6451	–
${}^{85}_{\Lambda}$Mo	22.7663	${}^{86}_{\Lambda\Lambda}$Mo	49.0756	3.5615	–
${}^{89}_{\Lambda}$Ru	22.8877	${}^{90}_{\Lambda\Lambda}$Ru	49.2448	3.4694	–
${}^{93}_{\Lambda}$Pd	23.0167	${}^{94}_{\Lambda\Lambda}$Pd	49.4242	3.3908	–
${}^{97}_{\Lambda}$Cd	23.1202	${}^{98}_{\Lambda\Lambda}$Cd	49.5244	3.2840	–
${}^{101}_{\Lambda}$Sn	23.2215	${}^{102}_{\Lambda\Lambda}$Sn	49.6575	3.2145	–

$a = 0.6$ fm and $R = 1.1A^{\frac{1}{3}}$ fm. The depth of the core-Λ potential was adjusted to reproduce the single-Λ BE (B_Λ). The $\Lambda\Lambda$ and core-Λ potentials used by Yamamoto *et al* [67,68] are

$$\left.\begin{aligned} V_{\Lambda\Lambda}(r) &= \textstyle\sum_{i=1}^{3} v_i \exp(-(\frac{r}{\beta_i})^2) \\ V_{\Lambda c}(r) &= \dfrac{v_0}{1+\exp(\frac{r-R}{a})} \end{aligned}\right\}. \tag{45}$$

The parameters of the $\Lambda\Lambda$ potential are given in table 8. They calculated the two-Λ separation energy $B_{\Lambda\Lambda}$, $\Lambda\Lambda$ bond energy $\Delta B_{\Lambda\Lambda}$, the r.m.s. $\Lambda\Lambda$ radius ($R_{\Lambda\Lambda}$) and r.m.s. $\Lambda\Lambda$-core radius ($R_{(\Lambda\Lambda)c}$). The results are presented in table 9. Results of some other workers which are available are also presented in table 9. As evident from table 9, the observables of ${}^{14}_{\Lambda\Lambda}$C and ${}^{10}_{\Lambda\Lambda}$Be calculated by Yamamoto *et al* [67,68] for D2, WS are close to our result. However, their results for ${}^{6}_{\Lambda\Lambda}$He differ from those of our calculations which are due to the

Table 6. The r.m.s. matter radii and correlation co-efficient for different double Λ-hypernuclei at $K_{\max} = 20$.

Hypernuclei	r.m.s. radii (fm)						η
	R_A	$R_{c\Lambda}$	$R_{\Lambda\Lambda}$	$R_{(\Lambda\Lambda)c}$	$R_c^{\rm CM}$	$R_\Lambda^{\rm CM}$	
${}^{6}_{\Lambda\Lambda}$He	2.0207	2.4129	2.9340	1.9158	0.7145	1.8961	0.3329
${}^{10}_{\Lambda\Lambda}$Be	2.1905	2.1584	2.7035	1.6825	0.3857	1.8734	0.3116
${}^{14}_{\Lambda\Lambda}$C	2.4441	2.0281	2.5638	1.5716	0.2600	1.8340	0.3034
${}^{18}_{\Lambda\Lambda}$O	2.6841	1.9966	2.5321	1.5438	0.1998	1.8464	0.3000
${}^{22}_{\Lambda\Lambda}$Ne	2.8984	2.0191	2.5623	1.5601	0.1659	1.8938	0.2989
${}^{26}_{\Lambda\Lambda}$Mg	3.0883	2.0477	2.5970	1.5833	0.1428	1.9394	0.2985
${}^{30}_{\Lambda\Lambda}$Si	3.2593	2.0827	2.6421	1.6102	0.1261	1.9869	0.2982
${}^{34}_{\Lambda\Lambda}$S	3.4150	2.1170	2.6808	1.6386	0.1134	2.0305	0.2985
${}^{38}_{\Lambda\Lambda}$Ar	3.5583	2.1510	2.7211	1.6660	0.1033	2.0720	0.2988
${}^{42}_{\Lambda\Lambda}$Ca	3.6912	2.1814	2.7558	1.6911	0.0949	2.1086	0.2990
${}^{46}_{\Lambda\Lambda}$Ti	3.8157	2.2186	2.8015	1.7205	0.0883	2.1509	0.2993
${}^{50}_{\Lambda\Lambda}$Cr	3.9382	2.4470	3.1469	1.8741	0.0885	2.3799	0.2993
${}^{54}_{\Lambda\Lambda}$Fe	4.0433	2.2853	2.8815	1.7739	0.0776	2.2256	0.2998
${}^{58}_{\Lambda\Lambda}$Ni	4.1483	2.3174	2.9202	1.7995	0.0733	2.2609	0.3001
${}^{62}_{\Lambda\Lambda}$Zn	4.2483	2.3499	2.9601	1.8253	0.0696	2.2963	0.3003
${}^{66}_{\Lambda\Lambda}$Ge	4.3439	2.3814	2.9985	1.8502	0.0663	2.3302	0.3005
${}^{70}_{\Lambda\Lambda}$Se	4.4355	2.4120	3.0361	1.8744	0.0634	2.3631	0.3007
${}^{74}_{\Lambda\Lambda}$Kr	4.5235	2.4417	3.0726	1.8979	0.0607	2.3949	0.3008
${}^{78}_{\Lambda\Lambda}$Sr	4.6087	2.4969	3.1499	1.9375	0.0588	2.4516	0.3009
${}^{82}_{\Lambda\Lambda}$Zr	4.6924	2.6449	3.3746	2.0368	0.0588	2.5999	0.3009
${}^{86}_{\Lambda\Lambda}$Mo	4.7752	2.9114	3.7822	2.2135	0.0610	2.8653	0.3006
${}^{90}_{\Lambda\Lambda}$Ru	4.8536	3.0750	4.0272	2.3241	0.0612	3.0291	0.3005
${}^{94}_{\Lambda\Lambda}$Pd	4.9299	3.2503	4.2888	2.4425	0.0616	3.2042	0.3003
${}^{98}_{\Lambda\Lambda}$Cd	4.9979	3.0414	3.9608	2.3083	0.0558	2.9993	0.3008
${}^{102}_{\Lambda\Lambda}$Sn	5.0658	2.9299	3.7798	2.2388	0.0520	2.8903	0.3011

use of different potential model. The difference in ΛΛ bond energy ($\Delta B_{\Lambda\Lambda}$) are significantly large since this observable is very sensitive to the choice of a particular ΛΛ potential. However the calculated r.m.s. radii do not differ much from our result. The results of Himeno *et al* [69] for ${}^{6}_{\Lambda\Lambda}$He for D2, ORG potential model are close to our results. From table 9, we see that our results are closer to the available experimental data. Recently Caro *et al* have attempted to derive an effective ΛΛ interaction and also predicted some of the structural and decay properties of double-Λ hypernuclei not discovered yet [70]. They presented their binding energy data as a plot of the ratio $B_{\Lambda\Lambda}/2B_\Lambda$ against $A^{\frac{1}{3}}$ ($B_\Lambda, B_{\Lambda\Lambda}$ are one and two-Λ separation energies and A is the mass of the core nucleus). A rough estimate of the binding energy for ${}^{42}_{\Lambda\Lambda}$Ca from the plot seems to be close to our result.

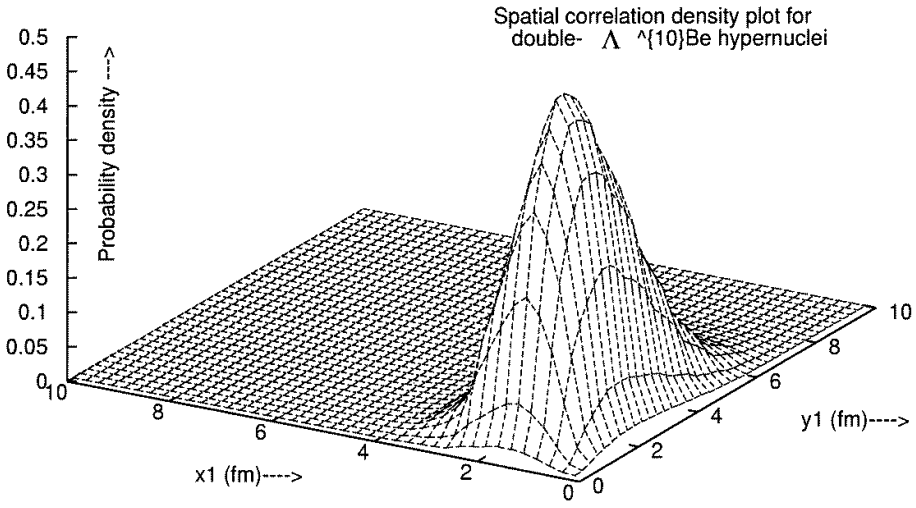

Figure 3. Spatial correlation density plot for the ground state of ${}^{10}_{\Lambda\Lambda}$Be in the $\Lambda\Lambda$ and $(\Lambda\Lambda)c$ variables (i.e., x_1, y_1 in fm).

4. Summary and conclusion

Since hyperons and nucleons both have three quark (qqq) structure (eg. $p \rightarrow uud$, $n \rightarrow udd$, $\Lambda^0 \rightarrow uds$ etc.) their interactions among themselves as well as with nucleons should give important inputs in the knowledge of strong interactions. But not much attention has so far been directed to the study of hyperon–hyperon and hyperon–nucleon interaction through the investigation of hypernuclei. We have undertaken a systematic study of the bound state properties of hypernuclei to shed light on the hyperon–hyperon and hyperon–nucleon interactions and the internal structure of the three body systems. The hyperspherical harmonics expansion (HHE) method adopted here is an essentially exact method, where calculations can be carried out up to any desired precision by gradually increasing the expansion basis. This can be seen in the first two columns of tables 3 and 4 where the binding energy gradually attains a convergence with increasing $K_{\max}$ values. It is also found from tables 3 and 4 that the convergence in the binding energy (with respect to increasing $K_{\max}$) is relatively slow, whereas the convergence rates for the other observables are faster. For ${}^{6}_{\Lambda\Lambda}$He, the calculated two-Λ separation energy $B_{\Lambda\Lambda}$ at $K_{\max} = 20$ (see table 3) and $\Lambda\Lambda$ bond energy $\Delta B_{\Lambda\Lambda}$ (see table 5) agrees fairly well with the experimental values 10.90 ± 0.50 MeV [2] and 4.70 ± 0.60 MeV [2] respectively within the allowed error limit. However the calculated $B_{\Lambda\Lambda}$ at $K_{\max} = 20$ (see table 4) and $\Delta B_{\Lambda\Lambda}$ (see table 5) for ${}^{10}_{\Lambda\Lambda}$Be are slightly greater than the experimental values 17.70 ± 0.40 MeV [1] and 4.30 ± 0.40 MeV [1] respectively. Although convergence in HH expansion is not fully attained with $K_{\max} = 20$, but since the exact data is only sketchy, we do not need high precision at this stage of the game. As discussed earlier the strength of the ΛN effective potential decreases as the mass (A_c) of the core nuclei increases (see table 2). A plot of the effective ΛN potential against the mass of the core (see figure 2) shows satura-

tion property in medium and heavy mass region ($A_c \geq 40$). In the mass region $A_c \leq 40$ the ΛN potential strength falls rapidly, while it falls relatively slowly in the mass region $A_c \geq 40$. The calculated two-Λ separation energy $B_{\Lambda\Lambda}$ shows saturation property in the heavy mass region and a relatively faster rise in the low mass region (see figure 2). As expected the r.m.s. matter radii increases as the mass A increases; however the calculated three body r.m.s. matter radii R_A are slightly smaller than the values $r_0 A^{1/3}$ for all the three body systems studied here. The calculted r.m.s. core Λ distance $R_{c\Lambda}$ (see third column of table 6) exhibit small oscillation with increasing mass. It decreases from the value 2.4129 fm at $A = 6$ to the value 1.9966 fm at $A = 18$, it then increases reaching a value 2.4470 fm at $A = 50$ which suddenly decreases to 2.2853 fm at $A = 54$ and again rises to 3.25 fm at $A = 94$. These anomalous values of $R_{c\Lambda}$ at masses $A = 18$, 54 and 98 indicate the possibility of existence of a relatively strong interaction of the valence

Table 7. The contribution of the orbital angular momenta l_{x_1} to the probability density in the ground state of different double Λ-hypernuclei at $K_{\max} = 20$.

Hypernuclei	Partial probability $P_{l_{x_1}}$ for l_{x_1}				
	0	1	2	3	4
${}^{6}_{\Lambda\Lambda}$He	0.996761	0.000000	0.003222	0.000000	0.000017
${}^{10}_{\Lambda\Lambda}$Be	0.998165	0.000000	0.001832	0.000000	0.000003
${}^{14}_{\Lambda\Lambda}$C	0.998994	0.000000	0.001006	0.000000	0.000001
${}^{18}_{\Lambda\Lambda}$O	0.999351	0.000000	0.000645	0.000000	0.000004
${}^{22}_{\Lambda\Lambda}$Ne	0.999501	0.000000	0.000491	0.000000	0.000007
${}^{26}_{\Lambda\Lambda}$Mg	0.999614	0.000000	0.000379	0.000000	0.000007
${}^{30}_{\Lambda\Lambda}$Si	0.999668	0.000000	0.000322	0.000000	0.000010
${}^{34}_{\Lambda\Lambda}$S	0.999727	0.000000	0.000264	0.000000	0.000009
${}^{38}_{\Lambda\Lambda}$Ar	0.999776	0.000000	0.000217	0.000000	0.000007
${}^{42}_{\Lambda\Lambda}$Ca	0.999849	0.000000	0.000150	0.000000	0.000001
${}^{46}_{\Lambda\Lambda}$Ti	0.999847	0.000000	0.000149	0.000000	0.000004
${}^{50}_{\Lambda\Lambda}$Cr	0.997843	0.000000	0.001901	0.000000	0.000255
${}^{54}_{\Lambda\Lambda}$Fe	0.999887	0.000000	0.000111	0.000000	0.000003
${}^{58}_{\Lambda\Lambda}$Ni	0.999905	0.000000	0.000094	0.000000	0.000002
${}^{62}_{\Lambda\Lambda}$Zn	0.999905	0.000000	0.000093	0.000000	0.000002
${}^{66}_{\Lambda\Lambda}$Ge	0.999911	0.000000	0.000087	0.000000	0.000002
${}^{70}_{\Lambda\Lambda}$Se	0.999915	0.000000	0.000084	0.000000	0.000002
${}^{74}_{\Lambda\Lambda}$Kr	0.999918	0.000000	0.000081	0.000000	0.000001
${}^{78}_{\Lambda\Lambda}$Sr	0.999628	0.000000	0.000347	0.000000	0.000025
${}^{82}_{\Lambda\Lambda}$Zr	0.998201	0.000000	0.001665	0.000000	0.000135
${}^{86}_{\Lambda\Lambda}$Mo	0.995102	0.000000	0.004548	0.000000	0.000350
${}^{90}_{\Lambda\Lambda}$Ru	0.993157	0.000000	0.006385	0.000000	0.000456
${}^{94}_{\Lambda\Lambda}$Pd	0.990907	0.000000	0.008524	0.000000	0.000564
${}^{98}_{\Lambda\Lambda}$Cd	0.994269	0.000000	0.005398	0.000000	0.000327
${}^{102}_{\Lambda\Lambda}$Sn	0.996127	0.000000	0.003666	0.000000	0.000203

Table 8. $\Lambda\Lambda$ potential depth v_i (MeV) in the $^1S_0$ state for each range β_i (fm). D, S and F denote those from model D, F and NSC respectively (from ref. [67]).

$i \rightarrow$	1	2	3
$\frac{\beta_i(\mathrm{fm}) \rightarrow}{v_i(\mathrm{MeV}) \downarrow}$	1.5	0.9	0.5
D1	−8.967	−226.80	880.7
D2	−8.951	−223.10	948.9
D3	−9.219	−242.70	1015.0
F1	−4.769	−091.72	675.7
F2	−4.825	−102.30	182.9
S1	−3.622	−045.81	136.4

Table 9. Comparison of our results with those obtained by other workers. D, F, S refer to Nijmegen $\Lambda\Lambda$ potential models, WS refers to Wood–Saxon core-Λ potential, YNG and ORG refer to folded core-Λ potentials.

System	Reference	Model	$B_{\Lambda\Lambda}$ (MeV)	$\Delta B_{\Lambda\Lambda}$ (MeV)	$R_{\Lambda\Lambda}$ (fm)	$R_{(\Lambda\Lambda)c}$ (fm)
${}^{6}_{\Lambda\Lambda}$He	Yamamoto [67]	D2,WS	9.50	3.24	3.17	2.07
	”	D3,WS	10.00	3.71	3.09	2.06
	Yamamoto [68]	D2,WS	9.50	3.24	3.17	2.07
	Himeno [69]	D2,YNG	9.00	2.8	3.20	2.06
	”	D2,ORG	10.90	4.6	2.59	1.58
	Present calc.		10.89	4.65	2.93	1.92
	Expt. [2]		10.90±0.50	4.70±0.60	–	–
${}^{10}_{\Lambda\Lambda}$Be	Yamamoto [67]	D1,WS	18.40	4.97	2.71	1.66
	”	D2,WS	17.70	4.26	2.79	1.67
	”	F1,WS	13.60	0.16	3.35	1.78
	”	F2,WS	17.70	4.26	2.71	1.66
	”	S1,WS	14.70	1.28	3.13	1.73
	Yamamoto [68]	D2,WS	17.70	4.26	2.79	1.67
	Himeno [69]	D2,WS	17.40	4.0	2.79	1.64
	”	F1,WS	13.20	−0.2	3.29	1.72
	Present calc.		18.86	5.43	2.70	1.68
	Expt. [1]		17.70±0.40	4.30±0.40	–	–
${}^{14}_{\Lambda\Lambda}$C	Yamamoto [67]	D2,WS	28.00	4.63	2.67	1.56
	Yamamoto [68]	D2,WS	28.00	4.63	2.67	1.56
	Present calc.		28.43	5.98	2.56	1.54
	Expt.		–	–	–	–

Λ hyperons with the core nucleons. The computed values of the partial probabilty (see table 7) shows that more than 90% of the contribution to the probability density comes from the $l_{x_1} = 0$ partial wave and the rest from the higher even l_{x_1} components. The contributtion from the odd values of l_{x_1} are zero. A relatively small value (~ 0.32) (see tables 3, 4 and 6) of the calculated correlation coefficient and the probability density plot indicate that the valence hyperons are not correlated.

Thus we conclude that the ground state wave function of all the above double Λ hypernuclei are an admixture of S, D, G partial waves and the effective ΛN interaction (between a N embedded in the core and a valence Λ) can be represented by a single term attractive Gaussian, whose strength decreases with increasing core mass (A_c). A smooth dependence on A_c over the entire mass range has been found. The gradual decrease in the strength may be viewed as the effect of screening of the interacting nucleon embedded in the core, by the surrounding nucleons. One intuitively expects such a result. As A_c increases, the valence Λ particles are gradually surrounded by other nucleons and effective ΛN interaction attains its saturation value.

Acknowledgement

Part of the calculation was done on computers provided by the Departmental Special Assistance (DSA) of the University Grants Commission (UGC), India.

References

[1] M Danysz *et al*, *Nucl. Phys.* **49**, 121 (1963)
[2] D J Prowse, *Phys. Rev. Lett.* **17**, 782 (1966)
[3] R H Dalitz, D H Davis, P H Fowler, A Montwill, J Poriewski and J A Zakrzewski, *Proc. R. Soc. London Ser.* **A426**, 1 (1989)
[4] S Aoki *et al*, *Prog. Theor. Phys.* **85**, 1287 (1991)
[5] A Gal, Advances, in *Nucl. Phys.* edited by M Baranger and E Vogt (Plenum, 1975) vol. 8, p. 1
[6] G Alexander *et al*, *Phys. Rev.* **173**, 1452 (1968)
[7] B Sechi-Zorn *et al*, *Phys. Rev.* **175**, 1735 (1968)
[8] J A Kadyk *et al*, *Nucl. Phys.* **B27**, 13 (1971)
[9] J M Hauptman, LBL Report No. LBL-3608 (1974)
[10] F Eisele *et al*, *Phys. Lett.* **B37**, 204 (1971)
[11] R Engelmann *et al*, *Phys. Lett.* **21**, 487 (1966)
[12] Y C Tang and R C Herndon, *Nuovo Cimento* **XLVIB (N1)**, 117 (1966)
[13] R H Dalitz and G Rajasekaran, *Nucl. Phys.* **50**, 450 (1964)
[14] A R Ali and A R Bodmer, *Phys. Lett.* **B24**, 343 (1967)
[15] A R Bodmer, Q N Usmani and J Carlson, *Nucl. Phys.* **A422**, 510 (1984)
[16] K Ikeda, H Bando and T Motoba, *Prog. Theor. Phys. (Suppl.)* **81**, 147 (1985)
[17] C D Lin, *Phys. Rep.* **257**, 1 (1995)
[18] T H Gronwall, *Phys. Rev.* **51**, 655 (1937)
[19] C D Lin, *Phys. Rev.* **A29**, 1019 (1984)
[20] C D Lin, *Phys. Rev. Lett.* **51**, 1348 (1983)
[21] J Macek, *J. Phys.* **B1**, 831 (1968)
[22] C H Greene, *Phys. Rev.* **A23**, 661 (1981)
[23] C D Lin, Xian-Hui Liu, *Phys. Rev.* **A37**, 2749 (1988)
[24] H Fakuda, T Ishihura and S Hara, *Phys. Rev.* **A41**, 1455 (1990)
[25] A M Launay and M Le Dourneuf, *J. Phys.* **B15**, 455 (1982)
[26] J L Ballot and J Navarro, *J. Phys.* **B8**, 172 (1975)
[27] R C Whitten and J S Sims, *Phys. Rev.* **A9**, 1586 (1974)
[28] R M Shoucri and B T Darling, *Phys. Rev.* **A12**, 2272 (1975)
[29] V B Mandelzweig, *Phys. Lett.* **A78**, 25 (1980)

[30] V D Efros, A M Frolov and M I Mukhtarova, *J. Phys.* **B15**, 1819 (1982)
[31] T K Das, R Chattopadhyay and P K Mukherjee, *Phys. Rev.* **A50**, 3521 (1994)
[32] R Chattopadhyay, T K Das and P K Mukherjee, *Phys. Scr.* **54**, 601 (1996)
[33] R Chattopadhyay and T K Das, *Phys. Rev.* **A57**, 1281 (1997)
[34] Md A Khan, S K Datta and T K Das, *Fizika (Zagreb)* **B8(4)**, 469 (1999)
[35] T K Das, H T Coelho and M Fabre de la Ripelle, *Phys. Rev.* **C26**, 2288 (1982)
[36] H T Coelho, T K Das and M Fabre de la Ripelle, *Phys. Lett.* **B109**, 255 (1982)
[37] T K Das and H T Coelho, *Phys. Rev.* **C26**, 754 (1982)
[38] S Bhattacharya, T K Das, K P Kanta and A K Ghosh, *Phys. Rev.* **C50**, 2228 (1994)
[39] M A Khan, S K Dutta, T K Das and M K Pal, *J. Phys.* **24**, 1519 (1998)
[40] Yu A Simonov, *Yad Fiz* **3**, 630 (1960) [*Sov. J. Nucl. Phys.* **3**, 461 (1960)]; in *Proceedings of the International Symposium on the Present Status and Novel Developments in the Nuclear Many Body Problem*, Rome, 1972 edited by F Calogena and C Ciofi Degli Atti (Editrice Composition, Bologna, 1973), p. 527; *Sov. J. Nucl. Phys.* **7**, 722 (1968)
[41] F Zernike and H C Brinkman, *Proc. Kon. Acad. Wtensch* **33**, 3 (1975)
[42] M Fabre de la Ripelle, *Proc. Int. Sch. Nucl. Theor. Phys.* (Predeal, 1969)
[43] M Fabre de la Ripelle, *Comp. Reend. Acad. Sci.* **B269**, 80 (1970); **A273**, 1007 (1971)
[44] G Erens, J L Visschers and R Van Wageningen, *Ann. Phys.* **67**, 461 (1971)
[45] J L Ballot, *Z. Phys. (Germany)* **A302**, 347 (1981); *Few Body System Suppl. (Austria)* **1**, 146 (1986)
[46] J L Ballot and M Fabre de la Ripelle, *Ann. Phys. (NY)* **127**, 62 (1980)
[47] J M Richard, *Phys. Rep.* **212**, 1 (1992)
[48] H Leeb, H Fiedeldey, E G O Gavin, S A Sofianos and R Lipperheide, *Few Body Systems* **12**, 55 (1992)
[49] N Barnea and A Novoselsky, *Ann. Phys. (NY)* **256**, 192 (1997)
[50] S Watanabe, Y Hosoda and D Kato, *J. Phys.* **B26**, L495 (1993)
[51] B R Johnson, *J. Chem. Phys.* **69**, 4678 (1978)
[52] A K Ghosh and T K Das, *Fizika* **22(3)**, 521 (1990)
[53] M Abramoitz and I A Stegun, *Handbook of Mathematical Functions* (Dover Publications, NY, 1970) (ninth printing) p. 774
[54] J Raynal and J Revai, *Nuovo Cimento* **68**, 612 (1970)
[55] T B De and T K Das, *Phys. Rev.* **C36**, 402 (1987)
[56] T K Das, H T Coelho and M Fabre de la Ripelle, *Phys. Rev.* **C26**, 2281 (1982)
[57] Y Yamamoto and H Bando, *Prog. Theor. Phys. Suppl.* **81**, 9 (1985)
[58] Y Yamamoto, T Motoba, H Himeno, K Ikeda and S Nagata, *Prog. Theor. Phys. Suppl.* **117**, 361 (1994)
[59] M M Nagets, T A Rijken and J J deSwart, *Phys. Rev.* **D15**, 547 (1977); **D20**, 1633 (1979)
[60] R H Dalitz, *Phys. Rev.* **112**, 605 (1958)
[61] R H Dalitz and L Liu, *Phys. Rev.* **116**, 1312 (1959)
[62] M M Block and R H Dalitz, *Phys. Rev. Lett.* **11**, 96 (1963)
[63] J B Adams, *Phys. Rev.* **156**, 1611 (1967)
[64] C Y Chung, D P Heddle and L S Kisslinger, *Phys. Rev.* **C27**, 335 (1983)
[65] B H Mc Kellar and B F Gibson, *Proc. Int. Conf. on Hypernuclear and Kaon Physics* Heidelberg, 1982 edited by B Povh, p. 156; *Phys. Rev.* **C30**, 322 (1984)
[66] M May *et al*, *Phys. Rev. Lett.* **47**, 1106 (1981)
[67] Y Yamamoto *et al*, *Prog. Theor. Phys.* **86**, (1991), 867
[68] Y Yamamoto, *Nucl. Phys.* **A547**, 233c (1992)
[69] H Himeno *et al*, *Prog. Theor. Phys.* **89**, 109 (1993)
[70] J Caro *et al*, *Nucl. Phys.* **A646**, 299 (1999)